Journal of Materials Chemistry A

Accepted Manuscript

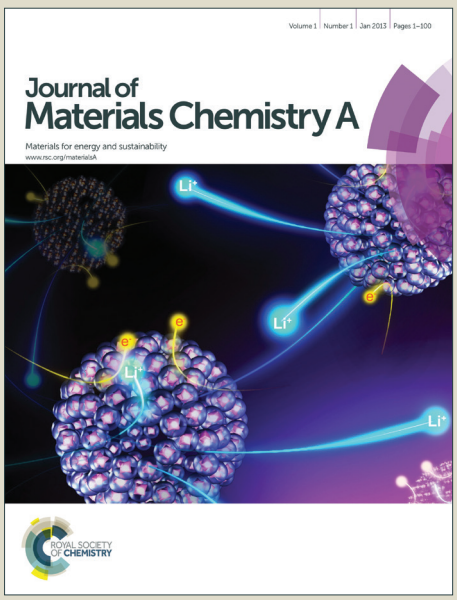

ROYAL SOCIETY OF CHEMISTRY

www.rsc.org/materialsA

Cite this: DOI: 10.1039/c0xx00000x

www.rsc.org/xxxxxx

ARTICLE TYPE

Sustainable photocatalytic production of hydrogen peroxide from water and molecular oxygen

Niv Kaynan,[a] Binyamin Adler Berke,[a] Ori Hazut[a] and Roie Yerushalmi*[a]

Received (in XXX, XXX) Xth XXXXXXXXX 20XX, Accepted Xth XXXXXXXXX 20XX

DOI: 10.1039/b000000x

We report the direct production of H_2O_2 from O_2 and H_2O by a heterogeneous catalyst made from non-toxic materials using light as the sole energy source for the process. Photocatalytic production of H_2O_2 is demonstrated using light energy without the need for additional chemical energy (sacrificial compounds) or applied electrical potential. Fine-tuning of catalyst architecture and interface design enables the exceptional photocatalytic activity.

Broader Context

H_2O_2 is a useful chemical reagent with numerous uses in the chemical industry, as a disinfectant, and as an environmentally friendly chemical fuel. Ideally, the production of H_2O_2 would utilize environmentally compatible materials throughout the process including the preparation of the catalyst and the reagents consumed. Furthermore, it is desirable to use sustainable energy resources such as available light energy for driving the process without additional energy required in the form of external electrical potential or chemical fuels. Namely, the ideal process may rely on photocatalytic producing of H_2O_2 by directly harnessing the excited hole-electron pair (exciton) for reducing molecular oxygen and oxidizing water molecules. However, until now all studies where direct photocatalytic production of H_2O_2 was attempted using non-toxic materials such as TiO_2 and gold or other environmentally compatible oxides without the use of hole scavengers showed only negligible concentrations. Our work demonstrate that the reactivity of well studied materials can be greatly enhanced by careful design of the catalyst architecture at the nano scale and meticulous interface design to improve overall charge separation and surface reactivity. The high level of control is achieved by relying on molecular layer deposition (MLD) for creating a metal oxide-organic hybrid thin film that is activated by a thermal anneal process. The controlled activation allows fine control of the catalyst properties including molecular permeability that plays a major role in the subsequent synthesis steps. The principles demonstrated here for TiO_2-Au-Si hybrid structures may be extended to other systems as well.

Hydrogen Peroxide (H_2O_2) is a widely used chemical in many synthetic pathways. Although H_2O_2 is an environmentally friendly compound, the production processes often involve the use of organic compounds and by-products that are not desirable. Numerous approaches have been studied and developed for production of H_2O_2 including the anthraquinone oxidation (AO) process, electrochemical processes, photocatalytic processes, and photoelectrochemical processes.[1-5] Specifically, photocatalytic generation of H_2O_2 is widely studied as a promising method for utilizing light energy to generate H_2O_2 as a useful chemical reagent and as an environmentally friendly chemical fuel by transforming light energy to chemical energy. It is desirable that such processes will utilize environmentally compatible materials for the preparation of the photocatalyst as well. Namely, the ideal photocatalytic process for producing H_2O_2 directly harnesses the excited hole-electron pair (exciton) for reducing molecular oxygen and oxidizing water molecules without the need for additional energy sources, such as externally applied electrical potential or chemical fuel. Metal oxides (MOs) and TiO_2-Au hybrid systems in particular have been widely studied as promising candidates in the context of photocatalytic production of H_2O_2 owing to their high stability and low toxicity.[6,7,8,9] However, until now all studies where direct photocatalytic production of H_2O_2 by MOs was attempted without the use of hole scavengers showed negligible concentrations.[6,10]

Namely, despite the vast ongoing research activity in this field there are no studies reporting the direct photocatalytic production of H_2O_2 by MOs without the consumption of organic compounds that act as sacrificial electron donors or the application of external electric field that provide the additional energy required for completing the photocatalytic reaction. Recently, a homogeneous photocatalytic system exhibiting direct generation of H_2O_2 from O_2 and H_2O was demonstrated using a Ru complex with the additional use of iridium oxide and rare earth metals ions as co-catalysts.[11]

Here we report the direct production of H_2O_2 from O_2 and H_2O by a heterogeneous catalyst made from non-toxic materials such as TiO_2, silicon and gold without using any external source of energy except for light. While the materials used are conservative, the catalyst structure exhibits a unique architecture resulting in the exceptional photocatalytic activity. Molecular layer deposition (MLD) of titanium ethylene glycol (Ti-EG) shell and subsequent thermal activation is used to produce the photo-active layer.[12] Addition of rare earth metal ions function as co-

catalysts further increasing the levels of H_2O_2 photocatalytically produced from O_2 and H_2O without using sacrificial compounds.

Briefly, the catalyst was synthesized using silicon nanowires (SiNWs) scaffolds prepared by chemical vapor deposition (CVD) and coated with titanium ethylene glycol (Ti-EG) shell by MLD to form core-shell structures (SiNW-Ti-EG). A thermal anneal step was applied for activating the Ti-EG layer resulting in a highly photocatalytic and molecularly permeable TiO_2 shell.[12] The thermal anneal of the Ti-EG layer results in decomposition of the organic components of the Ti-EG film and formation of TiO_2 nanocrystals with an anatase phase embedded in an amorphous layer, in agreement with our previous work[12] (see ESI for additional details and Table S1 for electron diffraction data).

Finally, the annealed core-shell structures were modified in solution for depositing gold clusters yielding SiNW-$(Ti\text{-}EG)_{anneal}$-Au structures. Quartz slides were used as UV transparent substrates for preparing catalyst films used for photocatalysis experiments (Fig. 1).

The photoactive TiO_2 shell preparation relies on thin Ti-EG films prepared by MLD followed by thermal activation step. This route provides an initially metastable organic-inorganic titanicone film as source for the TiO_2 shells that can be further tuned by annealing and chemically modifying steps while controlling critical properties such as the overall catalyst architecture, shell permeability, crystallinity and surface composition as will be discussed and demonstrated here (*vide infra*). This approach delivers fine control over a number of the critical factors that determines the overall photoreactivity of the hybrid catalyst resulting in the enhanced reactivity reported here. Most importantly, direct production of H_2O_2 from O_2 and H_2O require that the excited electron energy level is sufficient to promote electron transfer from the photocatalyst conduction band (CB) to the oxygen molecule. In addition, the hole oxidative potential, determined by the valence band (VB) position, should exceed the water oxidation potential.[13-15] The photoinduced reduction and oxidation processes are linked, so hampering any one of the processes result in charge accumulation and halting of the whole photocatalytic process. When both processes occur in tandem with sufficient efficiency, direct photocatalytic production of H_2O_2 can occur. Most studies related to photocatalytic generation of H_2O_2 report the use of hole scavengers that function as electron donors for completing the photocatalytic cycle or utilize externally applied electric potential.[16,17] Typically, the electron donors are sacrificial organic molecules that are consumed in the process and function as chemical fuel generating by-products. Additionally, the sacrificial compounds often results in partially or fully oxidized organic compounds and intermediates that are both environmentally unwanted and negatively interfere with the catalyst by adsorption to the catalyst surface and often result in catalyst passivation.[18] Such processes are less attractive as compared to a purely photocatalytic process that consumes only light, water and oxygen.

Illuminating the core-shell SiNW-$(Ti\text{-}EG)_{anneal}$-Au catalyst films suspended in acidic water (pH~2, HCl) showed direct formation of H_2O_2 without the addition of sacrificial compounds. H_2O_2 production was studied for various catalyst preparation conditions spanning MLD layer thickness between 4.5±1 and 13±2 nm corresponding to 25 to 80 cycles, respectively, and for an anneal range of 380 to 780 °C. In addition, the photocatalytic process was studied using UV (365 nm) and sun simulator illumination (AM 1.5G), (Fig. 2).

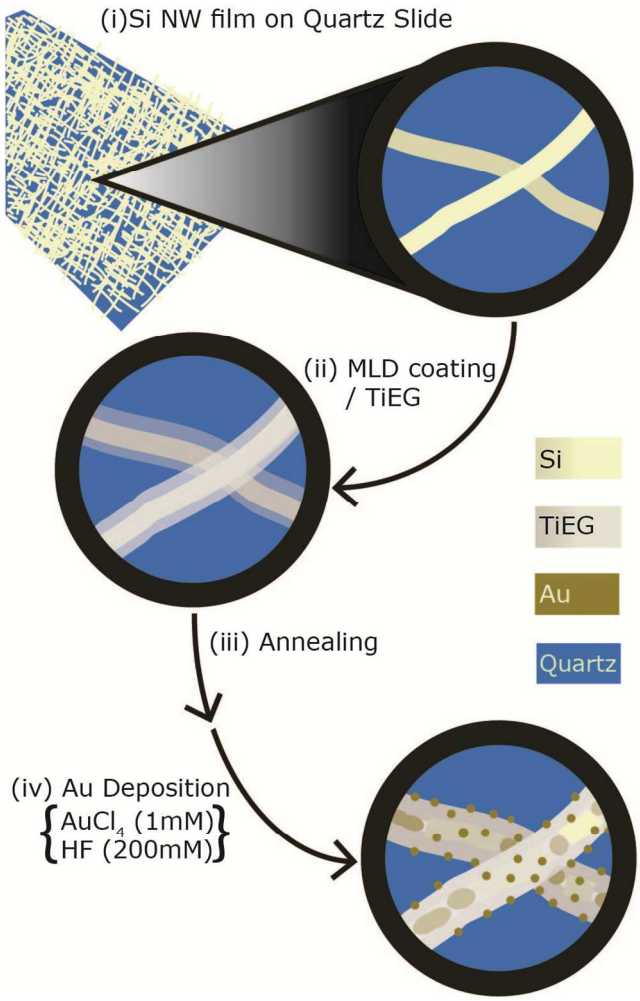

Fig. 1 Schematic description of catalyst preparation: (i) Silicon nanowire (NW) film is prepared on a quartz slide, (ii) coating of the NW structures by Ti-EG film formed by MLD, (iii) thermal anneal, and (iv) gold deposited at the annealed Ti-EG external and internal surfaces by galvanic displacement and photoinduced processes. The galvanic displacement process results in a partially hollow structure where the Si core is oxidized to SiO_2 and dissolved by the HF.

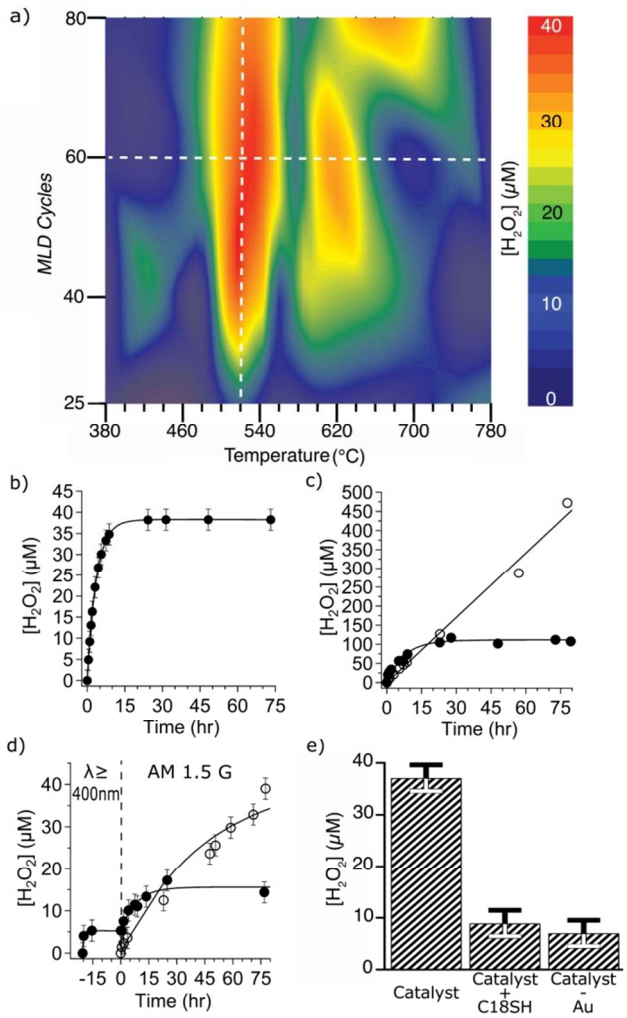

Fig. 2 Photocatalytic generation of H_2O_2. (a) Contour plot of maximal steady state concentration (SSC) of H_2O_2 obtained for catalyst preparation at various anneal temperatures and MLD cycles. XPS analysis is available for catalyst conditions along the broken lines (*vide infra*). (b) Typical H_2O_2 evolution (illumination: 365 nm, catalyst: 60 MLD cycles, 520 °C anneal). (c) Effect of addition of co-catalyst, $Y(NO_3)_3$, 25 mM (●) , and $Sc(NO_3)_3$ 6mM (○). (d) Visible light (λ≥400nm) and simulated sun (AM 1.5G) production of H_2O_2 with $Y(NO_3)_3$, 25 mM (●) , and $Sc(NO_3)_3$ 6mM (○), and (e) H_2O_2 SSC for catalyst with as-deposited gold, gold blocked by long chain alkyl thiol (1-octanedecanethiol), and without gold deposition step. Line plots of SSC of H_2O_2 vs. anneal temperatures and MLD cycles for the data points along the dashed lines are provided in Figs. S1a and b, respectively.

The steady state concentration (SSC) of H_2O_2 depends on both the film thickness and anneal temperature with optimal values corresponding to 60 MLD cycles and an anneal temperature of 520 °C (Fig. 2a). The formation and decomposition of H_2O_2 follow zero- and first-order kinetics, respectively.[16,17,19] The kinetic data were modeled using equation 1: [16,17,19]

$$\left[H_2O_2\right]_t = \left(\frac{k_f}{k_d}\right)\left(1-\exp\left(-k_d t\right)\right) \qquad (1)$$

Where t is time, k_f and k_d are the formation and decomposition rate constants for H_2O_2, respectively, and k_f is expressed in (μM x h^{-1}) and k_d in (h^{-1}).

Typical evolution of H_2O_2 for optimal catalyst preparation parameters at UV illumination (365 nm) is presented in Fig. 2b (SSC of 38 μM, k_f = 10.5 μM x h^{-1} and k_d = 0.27 h^{-1}).

The addition of a rare earth co-catalyst (Y^{3+}) resulted in a dramatic increase in the SSC of H_2O_2 to 114 μM, (k_f = 14.8 μM x h^{-1}, and k_d = 0.13 h^{-1}). An even more dramatic increase in H_2O_2 concentration and change in the overall kinetics was obtained by adding Sc^{3+} as co-catalyst resulting in a steady linear increase and overall zero order kinetics (k_f = 5.7 μM x h^{-1}), Fig. 2c. Sc^{3+} cations have been shown to act as Lewis acid co-catalyst facilitating two-electron reduction of O_2 and effective inhibitors of disproportionation of H_2O_2.[11] The same catalyst samples were used for studying the reactivity under visible light (λ≥400nm) and simulated sun illumination (AM 1.5G) showing SSC of ~5 μM and ~15 μM, respectively (Fig. 2d) for Y^{3+}. Significantly higher concentrations of H_2O_2, above 40 μM, were obtained for AM 1.5G illumination in the presence of Sc^{3+}. Although the catalyst absorption spectra shows a clear plasmon band (Fig. S4) simultaneous catalyst illumination by UV and visible light sources showed no observable enhancement in the photocatalytic production rates or SSC of H_2O_2.

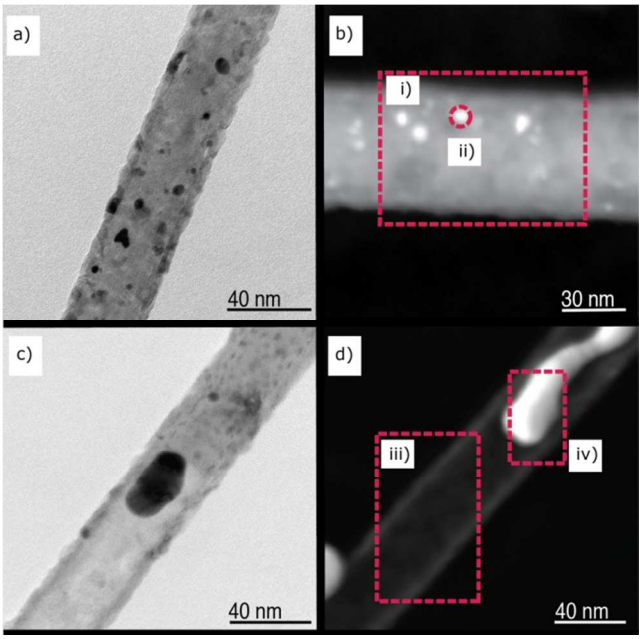

Fig. 3 Transmission electron microscopy (TEM) of SiNW-Ti-EG catalyst structures prepared at optimal process conditions (60 MLD cycles, anneal at 520 °C). (a) HRTEM images showing catalyst region with the SiNW core, TiO_2 shell and gold clusters deposited at the outer surface and (b) STEM images of similar region. (c) HRTEM images showing catalyst region with partially hollow TiO_2 tube coated and gold clusters deposited at the inner tube confinement, and (d) STEM image of similar region. EDS spectra and quantification for the corresponding regions highlighted with broken line frames are available in Fig. S3 and Table S2, respectively.

The role of gold clusters in the overall photocatalytic process was further studied by blocking the gold surface by a long-chain alkyl thiol (1-octanedienethiol) resulting in significantly lower SSC of H_2O_2, similar to the levels measured for catalyst without the gold deposition step (Fig. 2e). Our combined results suggest that the deposited gold clusters effectively improve charge

separation and assist in avoiding recombination reactions.[20-23]

In addition to the electronic effects, some aspects regarding O_2 and H_2O diffusion at the catalyst interface may have additional contributions as well. Photocatalysis experiments performed using deoxygenated solutions and measured under Ar did not result in significant SSC of H2O2 pointing at dissolved O2 as the source for oxygen in the reaction (Fig. S2). Previously we reported the enhanced photocatalytic activity of TiO_2 films obtained by annealing Ti-EG layers prepared by MLD which exhibit a molecularly permeable TiO_2 layer with unique properties distinct from TiO_2 films obtained by other preparation methods, such as atomic layer deposition (ALD).[14] In addition, several studies demonstrated the enhanced photocatalytic activity of SiNW-TiO_2 core-shell structures;[24-29] however direct photocatalytic production of H_2O_2 from O_2 and H_2O by a heterogeneous catalyst made from those materials, without the need for sacrificial compounds or externally applied potential was not reported. We suggest that the molecular permeability of the TiO_2 layer obtained by annealing the MLD film plays a significant role in the catalyst preparation and performance where gold is deposited onto the annealed SiNW-Ti-EG core-shell structure. The gold deposition step is performed in solution with both galvanic displacement (GD) and photocatalytic deposition (PD) taking place in the presence of HF and light. The simultaneous deposition by GD and PD resulted in mixture of full and hollow nanoarchitectures.

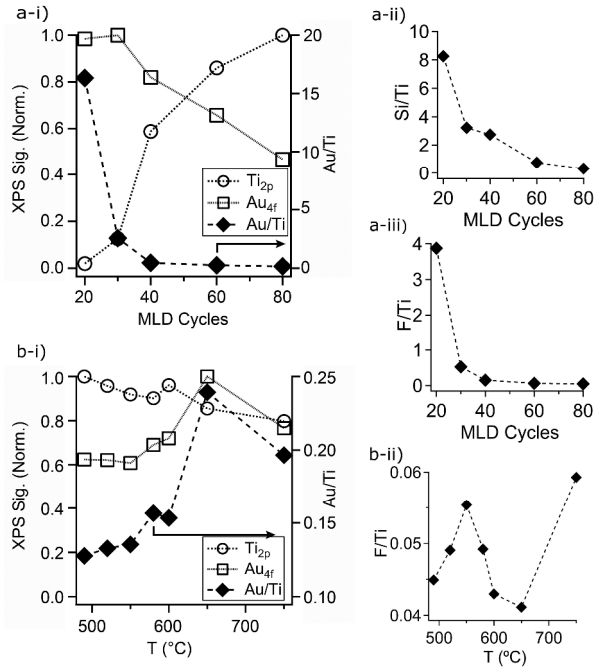

Fig. 4 Catalyst composition measured by X-ray photoelectron spectroscopy (XPS). (a) For increasing MLD cycles at constant temperature, 520°C, and (b) for increasing anneal temperature with constant Ti-EG film thickness (60 MLD cycles).

The filled nanoarchitectures comprise of SiNW core coated with permeable TiO_2 layer and decorated with gold clusters at the external surface (Fig. 3a,b). The hollow structures consist of a TiO_2 shell decorated with gold clusters at the outer surface and additional gold deposited inside the tube (Fig. 3c,d). The GD process occurs by diffusion of reactants through the permeable TiO_2 layer and oxidation of the Si core to SiO_2 yielding reduced metal clusters inside the core region. The resulting SiO_2 is dissolved by the HF and diffuses via the permeable TiO_2 layer leading to the partially hollow core with the pea-pod like structures. By varying the preparation parameters the distribution of hollow to filled structures can be tuned ranging from predominantly hollow pea-pod like structures with gold clusters in the internal surface to predominantly filled structures with the SiNW core retained and gold deposition at the external surface (Fig. S5). Maximal SSC of H_2O_2 is obtained for 60 MLD cycles and an anneal temperature of 520 °C. TEM analysis and X-ray photoelectron spectroscopy (XPS) characterization (vide infra) show at optimal catalyst preparation parameters a mixture of full and hollow structures decorated with gold clusters as described above. The permeable TiO_2 layer obtained by annealing the Ti-EG MLD film results in a gold-TiO_2 interface where the deposited gold is directly incorporated into the oxide not only at the nanotube surface as would be in the case of metal evaporation or attachment of preformed nanoparticles. This characteristic assists in enhancing Au-TiO_2 interfacial interactions that are critical for promoting charge separation at the interface.[30-32]

Catalyst composition was studied by XPS analysis for various MLD film thicknesses at constant anneal temperature of 520 °C and for various anneal temperatures for 60 MLD cycles. As expected, the Ti signal increases with number of MLD cycles (Fig. 4a-i). The Au signal decreases with MLD cycles because of screening of the XPS signal arising from Au clusters deposited inside the tubes with increasing tube wall thickness. Si/Ti and F/Ti atomic ratios decrease with the number of MLD cycles, as shown in Fig.s 4a-ii and 4a-iii, respectively.

For the various anneal temperatures, the Ti signal remains quite constant. In contrast, a sharp increase in Au/Ti atomic ratio is measured for 650 °C (Fig. 4b-i). We attribute the sharp increase in the Au/Ti ratio to the increase in photocatalytic activity of the annealed Ti-EG film at this temperature, leading to higher PD of gold, in accordance with previous work.[14] The XPS analysis demonstrates that the F/Ti ratio varies with temperature. In addition, F1s binding energy (BE) changes from 685.8 eV for thin MLD films up to 30 cycles to 684.3 eV for thicker MLD films (Fig. S6). This result suggests mainly Si-F and Ti-F species for thin and thick MLD layers, respectively. In addition, for optimal catalyst preparation conditions F1s BE corresponds to surface Ti-F species rather than F-doped TiO_2.[33-35] Numerous studies have shown that surface fluorination improves TiO_2 photocatalytic performance in general and for H_2O_2 and water oxidation processes in particular.[36-39] Thus, the gold deposition in the presence of HF not only results in deposition of gold clusters both inside and outside the TiO_2 shell for improving the charge separation, but also yields a beneficial Ti-F surface modification of the catalyst by the same process.

Conclusions

In conclusion, we have demonstrated the direct photocatalytic production of H_2O_2 from O_2 and H_2O by a heterogeneous catalyst made from non-toxic materials such as TiO_2, silicon and gold. Although the materials used are conventional, the photocatalyst exhibits unique architecture that results in the exceptional

photocatalytic activity. The unique hybrid structure design allows achieving this breakthrough using well studied materials such as TiO_2, Au and Si and further emphasizing the novelty of our approach. The unprecedented reactivity of the materials used in the hybrid structure is owing to exquisite control of the structure and interfaces rather than resorting to exotic compositions and materials. Future work will focus in improved visible light activity by utilizing the MLD layer properties for doping and possibly taking advantage of plasmon enhanced photoactivity.

Acknowledgements

We thank Dr. Vitaly Gutkin for XPS analysis. This work was partially funded by a starting grant from the European Research Council (ERC) under the European Community's Seventh Framework Programme Grant agreement no 259312 and by the Israel Science Foundation (ISF) under Grant (690/09).

Notes and references

[a] *Institute of Chemistry and The Center for Nanoscience and Nanotechnology, The Hebrew University of Jerusalem, Edmond J. Safra Campus, Givat Ram, Jerusalem, 91904Israel.*
E-mail: roie.yerushalmi@mail.huji.ac.il

† Electronic Supplementary Information (ESI) available: [Synthesis and characterization of the photocatalyst system.]. See DOI: 10.1039/b000000x/

1 S. Shibata, T. Suenobu, S. Fukuzumi, *Angew. Chem. Int. Ed*., 2013, **52**, 12327-12331.
2 S. Siahrostami, A. Verdaguer-Casadevall, M. Karamad, D. Deiana, P. Malacrida, B. Wickman, M. Escudero-Escribano, E. A. Paoli, R. Frydendal, T. W. Hansen, I. Chorkendorff, I.E. L. Stephens, J. Rossmeisl, *Nat. Mater.,* 2013, **12**, 1137-1143.
3 J. M. Campos-Martin, G. Blanco-Brieva, J. L. G. Fierro, *Angew. Chem. Int. Ed*., 2006, **45**, 6962-6984.
4 D. Hâncu, J. Green, E. J. Beckman, *Acc. Chem. Res.,* 2002, **35**, 757-764.
5 A. Fujishima, T. N. Rao, D. A. Tryk, *J. Photochem. Photobiol., C*, 2000, **1**,1-21.
6 C. Kormann, D. W. Bahnemann, M. R. Hoffmann, *Environ. Sci. Technol*., 1988, **22**, 798-806.
7 A. J. Hoffman, E. R. Carraway, M. R. Hoffmann, *Environ. Sci. Technol*., 1994, **28**, 776-785.
8 D. Jašin, A. Abu-Rabi, S. Mentus, D. Jovanović, *Electrochim. Acta*, 2007, **52**, 4581-4588.
9 C. Sivadinarayana, T. V. Choudhary, L. L. Daemen, J. Eckert, D. W. Goodman, *J. Am. Chem. Soc*., 2004, **126**, 38-39.
10 Y. Liu, J. Han, W. Qiu, W. Gao, *Appl. Surf. Sci*., 2012, **263**, 389-396.
11 S. Kato, J. Jung, T. Suenobu, S. Fukuzumi, *Energy Environ. Sci*., 2013, **6**, 3756-3764.
12 (a) S. Ishchuk, D. H. Taffa, O. Hazut, N. Kaynan, R. Yerushalmi, *ACS Nano*, 2012, **6**, 7263-7269; (b) See Sarkar D. et al. ,2014, for additional details regarding the permability and tunability of annealed Ti-EG layers.
13 X. Chen, S. Shen, L. Guo, S. S. Mao, *Chem. Rev*., 2010, **110**, 6503-6570.
14 A. Mills, S. Le Hunte, *J. Photochem. Photobiol., A*, 1997, **108**, 1-35.
15 M. R. Hoffmann, S. T. Martin, W. Choi, D. W. Bahnemann, *Chem. Rev*., 1995, **95**, 69-96.
16 D. Tsukamoto, A. Shiro, Y. Shiraishi, Y. Sugano, S. Ichikawa, S. Tanaka, T. Hirai, *ACS Catal*., 2012, **2**, 599-603.
17 M. Teranishi, S. Naya, H. Tada, *J. Am. Chem. Soc*., 2010, **132**, 7850-7851.
18 P. Sawunyama, A. Fujishima, K. Hashimoto, *Langmuir*, 1999, **15**, 3551-3556.
19 X. Li, C. Chen, J. Zhao, *Langmuir*, 2001, **17**, 4118-4122.
20 C. Yogi, K. Kojima, T. Hashishin, N. Wada, Y. Inada, E. Della Gaspera, M. Bersani, A. Martucci, L. Liu, T. Sham, *J. Phys. Chem. C,* 2011, **115**, 6554-6560.
21 A. Primo, A. Corma, H. García, *Phys. Chem. Phys*., 2011, **13**, 886-910.
22 I. Bannat, K. Wessels, T. Oekermann, J. Rathousky, D. Bahnenmann, M. Wark, *Chem. Mater*., 2009, **21**, 1645-1653.
23 V. Subramanian, E. E. Wolf, P. V. Kamat, *J. Am. Chem. Soc*., 2004, **126**, 4943-4950.
24 Y.Pu, G. Wang, K. Chang, Y.Ling, Y. Lin, B. C. Fitzmorris, C. Liu, X. Lu, Y, Tong, J, Z. Zhang, Y, Hsu, Y. Li, *Nano Lett*., 2013, **13**, 3817-3823.
25 L. Liu, Y. Cao, J. He, X. Qi, W. Shi, Q. Yang, *J. Nanosci. Nanotechnol*., 2013, **13**, 6835-6840.
26 Y. J. Hwang, C. Hahn, B. Liu, P. Yang, ACS Nano 2012, **6**, 5060-5069.
27 H. Yu, S. Chen, X. Quan, H. Zhao, Y. Zhang, *Appl. Catal., B*, 2009, **90**, 242-248.
28 Y. J. Hwang, A. Boukrai, P. Yang, *Nano Lett*., 2009, **9**, 410-415.
29 M. S. Sander, M. J. Côté, W. Gu, B. M. Kile, C. P. Tripp, *Adv. Mater*., 2004, **16**, 2052-2057.
30 X. Zhang, Y. L. Chen, R. Liu, D. P. Tsai, *Rep. Prog. Phys*., 2013, **76**, 046401-046401.
31 J. Ohyama, A. Yamamoto, K. Teramura, T. Shishido, T. Tanaka, *ACS Catal.*, 2011, **1**, 187-192.
32 S. J. Tauster, S. C. Fung, R. T. K. Baker, J. A. Horsley, *Sci*., 1981, **211**, 1121-1125.
33 A. M. Czoska, S. Livraghi, M. Chiesa, E. Giamello, S. Agnoli, G. Granozzi, E. Finazzi, C. Di Valentin,G. Pacchioni, *J. Phys. Chem. C*, 2008, **112**, 8951-8956.
34 H. Park, W. Choi, *J. Phys. Chem. B*, 2004, **108**, 4086-4093.
35 T. Yamaki, T. Sumita, S. Yamoto, *J. Mater. Sci. Lett*., 2002, **21**, 33-35.
36 G. Wu, A. Chen, *J. Photochem. Photobiol*., A 2007, **195**, 47-53.
37 H. Kim, W. Choi. *Appl. Catal., B*, 2007, **69**, 127-132.
38 V. Maurino, C. Minero, G. Mariella, E. Pelizzetti, *Chem. Commun*., 2005, 2627-2629.
39 C. Minero, G. Mariella, V. Maurino, E. Pelizzetti, *Langmuir*, 2000, **16**, 2632-2641.

The table of contents entry

Direct photocatalytic production of H_2O_2 is demonstrated using heterogeneous catalyst made from environmentally compatible materials and light energy without the need for additional chemical energy (sacrificial compounds) or applied electrical potential. Fine-tuning of catalyst architecture and interface design enables the exceptional photocatalytic activity.